Static and fatigue performance ofthick laminates test design and experimental compression results

Lahuerta, F.; Westphal, T.; Nijssen, R. P L; Van Der Meer, F. P.; Sluijs, L.J.

Publication date
2014

Document Version
Final published version

Published in
16th European Conference on Composite Materials, ECCM 2014

STATIC AND FATIGUE PERFORMANCE OF THICK LAMINATES TEST DESIGN AND EXPERIMENTAL COMPRESSION RESULTS

F. Lahuerta*[1], T. Westphal[1], R.P.L. Nijssen[1], F. P. van der Meer[2], L. J. Sluys[2]

[1]*Knowledge Centre WMC. Kluisgat 5, 1771 MV Wieringerwerf, The Netherlands*

[2]*Delft University of Technology, PO Box 5048,2600 GA Delft, The Netherlands*

* *Corresponding Author: f.lahuerta@wmc.eu*

Keywords: Compression test, FEM analyses, size effect, UD, fatigue

Abstract

The aim of this work is to study the thickness effect in static and fatigue tests of glass-fibre unidirectional compression coupons. For this purpose, the self-heating effect, the effect of specimen geometry, and the influence of the manufacturing processes have been minimized. A scaled thickness compression coupon has been designed with the intention of reducing the influence of geometrical differences and of the manufacturing process as the thickness is scaled. In addition the self-heating effect was controlled by tuning the test frequency. The coupon design was based on a finite element analysis. The development of the manufacturing process and the design of the gripping configuration are reported in the present work. Experimental data from static and fatigue tests are reported for 4, 10 and 20 mm thick coupons where the static allowables, elastic modulus, Poisson ratios and the R=10 S-N curves are compared in order to evaluate the thickness effect.

1. Introduction

Thick laminates are increasingly present in large composite structures such as wind turbine blades. Specifically cap and root sub-components can show thicknesses from 40-60 mm in a 40 meters long blade and up to 100-150 mm thick for a 100 meters blade. Generally, blade designs are based on static and fatigue coupon tests on 1-4 mm thick laminates. However, a thickness effect has been observed in limited available experimental data on thickness scaled multidirectional laminates (with dominant 0° plies), showing significantly shorter fatigue life in thick laminates under R=0.1 (tension) and R=-1 (tension / compression), and an ultimate tension strength reduction [1, 2].

Although there is some disagreement on the existence of a size effect in composites, different factors are suspected to play a role in the altered static and dynamic performance of thick laminates. These include the effect of self-heating [3] for dynamic loading, the scaling effect [4], and the manufacturing process influence [5]. These need to be clearly separated from e.g. the test conditions [6, 7] such as the gripping effects, the test fixture or the test method.

In addition to the ISO and ASTM compression standards, several compression test methods for coupon thicknesses between 1-5 mm can be found in literature. Different parameters have been taken into account, such as the tab taper angles [7], the tabbing material or configuration [8] and the shear-and-end combined loading [9].

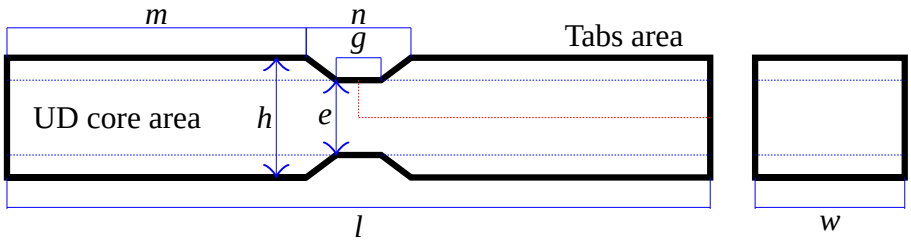

Figure 1: Scaled compression coupon parametric geometry, and dimensional parameters.

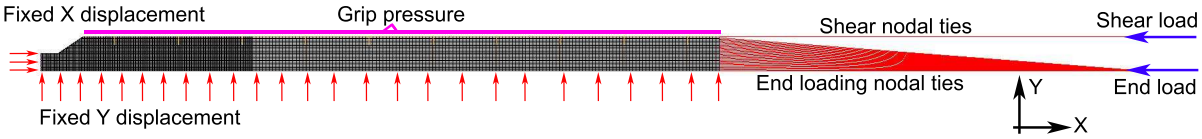

Figure 2: One quarter coupon model mesh and boundary conditions.

A few references are available in literature related to scaled compression tests on composites. Hsiao [9] performed static tests up to 10 mm thickness on UD (Unidirectional) carbon coupons observing no significant reduction of the ultimate strength. On the contrary, Soutis et al. [10] performed several series of carbon open-hole thickness-scaled static tests up to 8 mm observing a reduction of the ultimate strength. In addition Cordes [11] performed a series of compression tests on 10 mm thick specimens with different cross-ply lay-ups from which it was concluded that the static behaviour of the cross ply composites is dominated by the zero degree layers.

2. Scaled coupons parametric FEM design methodology

In order to engineer the scaled coupon geometries, a FEM parametric analysis was carried out using MSC Marc software. The geometry and relevant parameters are described in figure 1.

The parametric FEM analysis was performed for the 10 mm thick coupons. Based on case 0 dimensions (see figure 6) one geometrical parameter per case (see table 2) was modified in order to analyse the influence. One quarter of the coupon was simulated and two different meshes have been considered:

- 9072 2D four-node elements. With a maximum element length of 0.5 mm in the gauge section and initial tab area.
- A second equivalent mesh with cohesive elements between each laminate layer in order to consider tab delamination.

The model boundary conditions are shown in figure 2. A clamping surface grip pressure of 200 bar was used. The total load applied was 150 kN for a thickness (dimension e, figure 1) of 10 mm. The total load is distributed between the shear load and the end load based on an unknown distribution factor α according to equation (1). The distribution factor α is included in the parametric analysis in a range between 0.05 to 0.95.

$$F_{Total} = F_{End} + F_{Shear} \; ; F_{End} = (1 - \alpha) \cdot F_{Total} \tag{1}$$

Each ply is modelled with two rows of 2D solid elements with the orthotropic material properties given in table 1. Bilinear cohesive elements are used between each layer given in ta-

FEM	Modulus E [GPa]			Poisson [-]			Shear modulus G [GPa]		
Materials	11	22	33	11	22	33	11	22	33
UD	39.90	13.19	13.19	0.26	0.20	0.08	3.5	3.5	3.5
Biax(12)	25.00	25.00	13.10	0.15	0.15	0.08	3.5	3.5	3.5

	$G_I\,[kJ/m^2]$	$G_{II}\,[kJ/m^2]$	Critical opening $[\mu m]$	Max opening $[\mu m]$
Cohesive	1.25	4.00	5.41	29.4

Table 1: Materials and cohesive elements properties used in the FEM models.

Parameter	Cases	Values
g $[mm]$	0 / 1 / 2 / 3	5 to 40
n $[mm]$	0 / 4 / 5 / 6 / 7 / 8	14 to 50
l $[mm]$	0 / 9 / 10 / 11	225 to 525
α $[-]$	0 / 12 /13 /14 / 15	0.05 to 0.95
h $[mm]$	0 / 16 / 17 / 18	13 to 25

Table 2: Parametric cases.

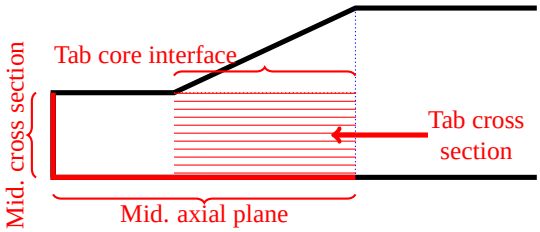

Figure 3: Stress failure index locations.

ble 1 properties. Prior to the simulations, cohesive properties were calibrated against Double-cantilever Beam (DCB) and End-notched Flexure (ENF) tests [12, 13].

In order to compare the different parametric cases, maximum stress failure indexes at the 95% percentile were considered for 4 different locations (see figure 3). The stress σ_x in the 11 laminate direction is studied at the middle cross section, the tab cross section, the tab / UD core interface and the middle xz axial plane. In addition, shear stress τ is studied at the tab / UD core interface and stress σ_y is evaluated in the middle cross section as an indicator for buckling of the outer layers.

3. Results and discussions. Scaled coupons parametric FEM design.

Stress gradients in the x-direction are shown in figure 4. Due to the specific loading the middle layers show lower stresses than the outer layers. The increase of the stresses in the outer core layers implies a decrease of the stresses in the middle core layers. The use of cohesive elements in between the layers reduces the stress gradients through the thickness in comparison with the non-cohesive simulations, but it does not cancel the effect. In addition, the cohesive elements damage index shows that in the tab / core interface, delamination occurs. This agrees with the location of the highest stress intensity.

The increase of the gauge section length (parameter g) reduces the through-thickness stress gradient (see figure 5, top-left) due to the fact that the mid cross section and tab cross section σ_x decrease with parameter g. In the same way the increase of parameter n related with the tab

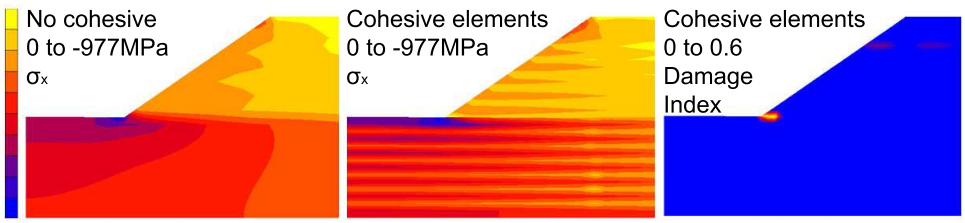

Figure 4: Stress profile and damage index in axial direction for cohesive and non-cohesive models.

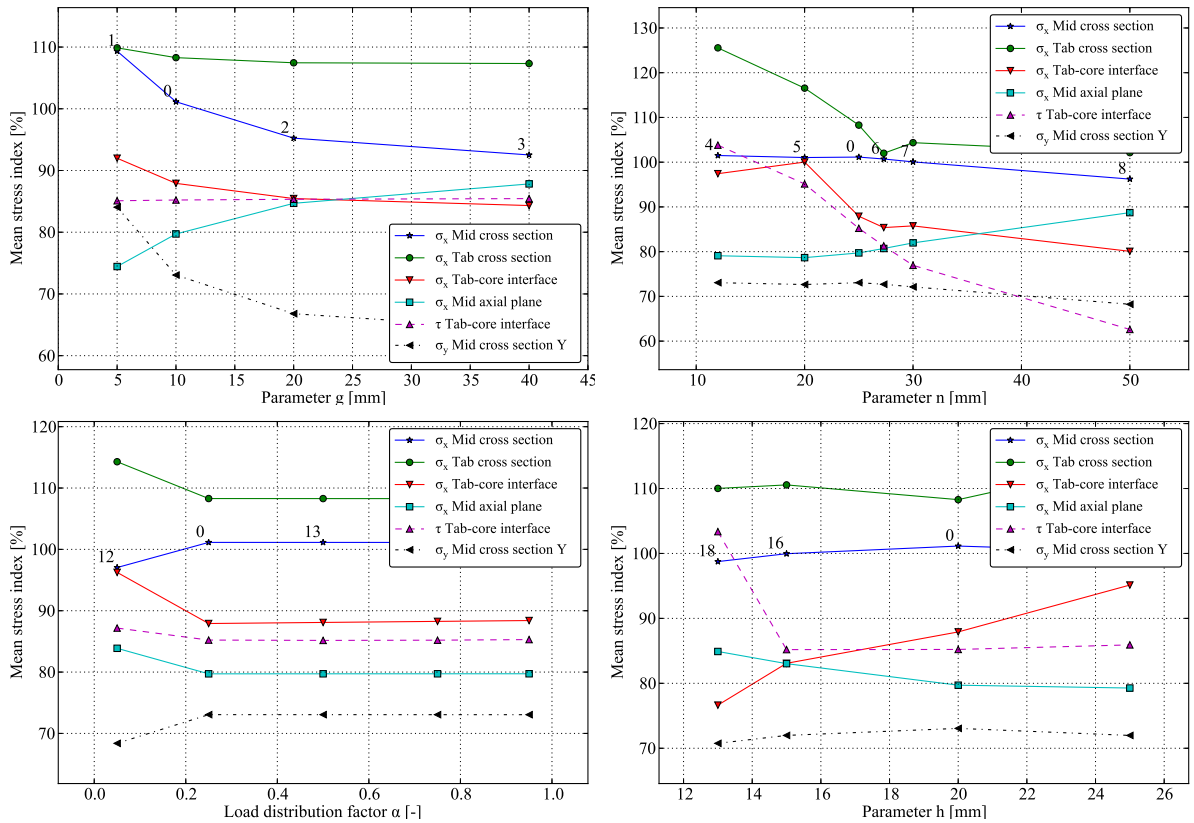

Figure 5: Main indicators of the FEM parametric analysis. Cohesive element models.

taper angle (see Figure 5, top-right), reduces the stress gradients through-the-thickness. In both cases the increase of the gauge section length and the reduction of the tab taper angle reduce the possibility of failure in the tab cross section and increase the possibility of failure at the gauge section. However, in both cases the possibility of buckling of the outer core layers in the gauge section increases due to the transverse displacements increase. In addition, the effects of the taper angle might evolve in time due to the growth of the damage or delamination in the tab / core interface predicted by the cohesive models.

The load distribution factor between the end load and the shear load implies a small increase of all indicators from a full end loading case to a full shear loading case (see figure 5, bottom-left). It has to be taken into account that in reality the load introduction by shear in a clamp is not evenly distributed as in the model due to the surface tolerances, surfaces roughness and grips marks. Thus, despite a full shear load case seems to be the most beneficial case according to the model, it is considered that a certain amount of end loading cancels the possibility of slippage in the grips and allows to freely setup the grip pressure. Moreover, the parameter h (see figure 5, bottom-right) related with the tab thickness shows that higher tab thicknesses influence the stress gradient through the thickness and reduce the shear in the tab core interface. Also the tab thickness increase slightly promotes the probability of failure in the tab cross section as the tab cross section σ_x index shows.

The optimal geometry chosen for experimental testing was case 0 which according to the models seems to be an average case between all different possibilities and can be clamped in the actual machines. Case 0 dimensions were scaled into case 22 and 23 shown in figure 6 with 4 and 20 mm thickness, respectively.

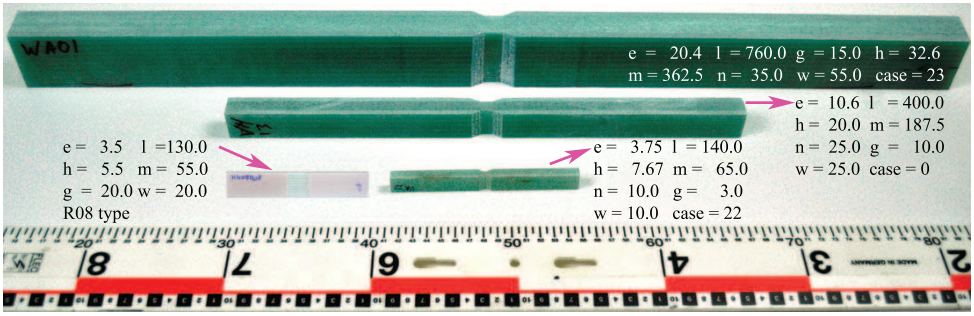

Figure 6: Thickness scaled compression coupon. Milled and R08 configuration. Dimensions in millimeters.

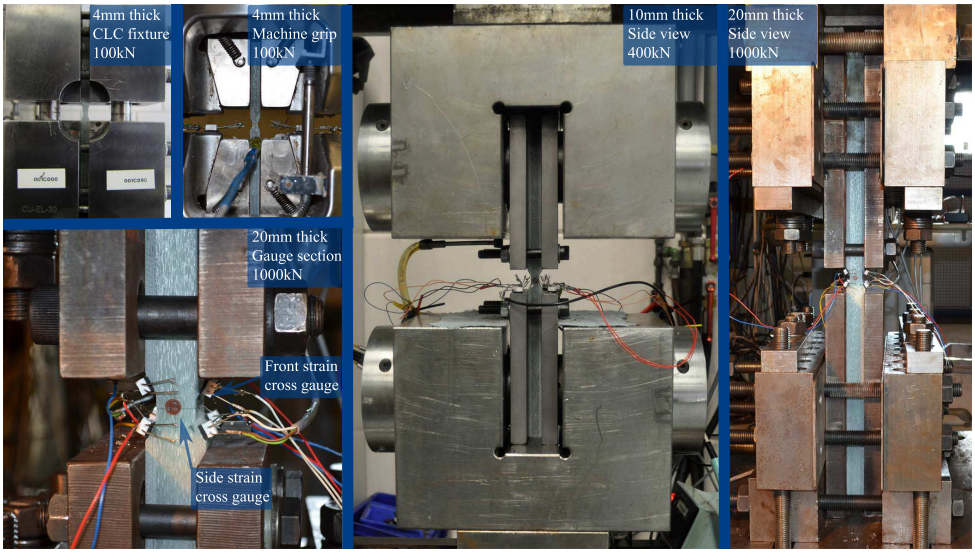

Figure 7: Test setup of 4, 10 and 20 mm coupons on 0.1, 0.4 and 1 MN servo-hydraulic test frames.

4. Experimental methodology

Several vacuum infused plates were manufactured with a commonly used wind energy epoxy resin (Hexion RIM135) and glass fibre (GFRP) type E. UD core was layout with unidirectional (UD) 600 gr/m^2 non-crimp fabric, and the tab area was layout with biaxial (70%) and 90° layers (30%). The plates were milled in thickness direction in order to create the gauge section and coupons were cut from the plate with a diamond saw (see figure 6). In addition, R08 type [14] rectangular 4 mm thick UD coupons with 20 x 20 mm gauge section and bonded tabs of 55 mm in length were prepared in order to compare these with the 4 mm milled thick coupons. For all manufactured plates the fibre content and glass transition temperature have been measured. The averaged fibre weight ratios were 70%, void content was under 0.1% and glass transition temperature (Tg) was around 80-85 °C.

Coupons with 4, 10 and 20 mm gauge section thickness were tested in static tests, and 4 and 10 mm thick coupons were tested in fatigue tests. The 4 mm coupons were tested in a MTS servo hydraulic 100 kN test frame, static tests were performed in a Combined Loading Compression (CLC) fixture according to ASTM D6641 and fatigue tests were performed with the standard machine grip system. Coupons of 10 and 20 mm thickness were tested on 400 kN and 1 MN test frames, respectively, equipped with an assembly of clamping steel plates (see figure 7).

The static tests were performed at 1 mm/min test speed. Tests at different bolt torques were carried out in order to find the optimal grip pressure. Fatigue tests were performed at 2 Hz

Bolt torque [Nm]		**e [mm]**	F_{max} [kN]	δ_{max} [mm]	σ_{max} [MPa]	E_{front} [GPa]	E_{sides} [GPa]	ν_{12} [−]	ν_{13} [−]	**Area $tested^*$ [cm^2]**
	Ref [14]	6.3			**577.4** (5.6%)	41.7 (1.1%)		0.301 (31.9%)		
6	VJ	3.5	28.1 (6.9%)	1.5 (11.3%)	**630.4** (4.8%)	-	-	-	-	2.7
40	VM	10.1	169.1 (4.0%)	4.9 (2.5%)	**649.6** (3.8%)	36.3 (12%)	46.1 (18%)	0.283 (12%)	0.198 (21%)	12.6
70	WH	19.1	691.4 (3.9%)	10.1 (2.1%)	**669.6** (1.2%)	41.9 (14%)	49.0 (5%)	0.235 (8%)	0.204 (14%)	41.7
3	VJ	3.5	24.0 (3.5%)	1.6 (10.1%)	**510.5** (3.3%)	-	-	-	-	2.7
<40	VM	10.3	133.9 (12.2%)	3.9 (17.7%)	**554.3** (10.2%)	34.0 (8%)	42.8 (11%)	0.297 (15%)	0.243 (26%)	12.8
30	WH	19.5	494.1 (9.5%)	8.1 (12.7%)	**479.9** (8.8%)	40.1 (12%)	44.4 (6%)	0.235 (6%)	0.175 (26%)	41.3

*Cross sectional area tested: is the width x thickness x number of coupons

Table 3: Experimental static results for 4, 10 and 20 mm thick coupons. Parenthesis values are the COVs.

(4 mm) and 1 Hz (10 mm) and monitored with thermocouples and infrared (IR) cameras in order to avoid surface temperatures over 30 °C. The 10 and 20 mm coupons were instrumented with cross gauges in the four gauge section faces in order to measure the elastic modulus in the outer surfaces and in the middle axial section. The use of cross gauges enabled measurement of Poisson coefficients ν_{12} and ν_{13}.

5. Results and discussions. Experimental tests.

It is well known that ultimate stresses in CLC type compression tests are influenced by the clamping pressure, thus tests for different thicknesses were carried out at two different clamping pressures. Table 3 shows that ultimate stresses can drop and show larger coefficients of variation (COV) when the clamping pressure is not optimal. However, in the cases with the optimal bolt torque the COVs were reduced and no thickness effect could be observed for the static ultimate strengths. Moreover, ultimate stresses show an increase with thickness combined with a reduction of the COVs. This increase could be related with the total amount of cross sectional area tested, as the amount of cross sectional area tested increase the statistical population gets more significant, so the COVs decrease and the ultimate strengths means shows a 6% increase.

The average elastic modulus from the front side surfaces and the lateral side surfaces are shown in table 3. Since the lateral side modulus corresponds to strain measurements in the middle axial section, they show higher values than the front modulus for the same thicknesses due to the stress gradient between the outer layers and the inner layers (see the FEM models). The same behaviour can be seen if elastic moduli are compared to the thickness increase. Because of this, thick laminate coupons do not allow the measurement of the elastic modulus due to the stress gradient that appear through the thickness. For measurement of the elastic modulus, thin coupons with ASTM D695 or DIN 65375 fixtures can be used.

On the other hand, because the cross sectional mean stress is not required in the Poisson ratio calculations from the cross gauge measurements, thick laminate coupons do allow the mea-

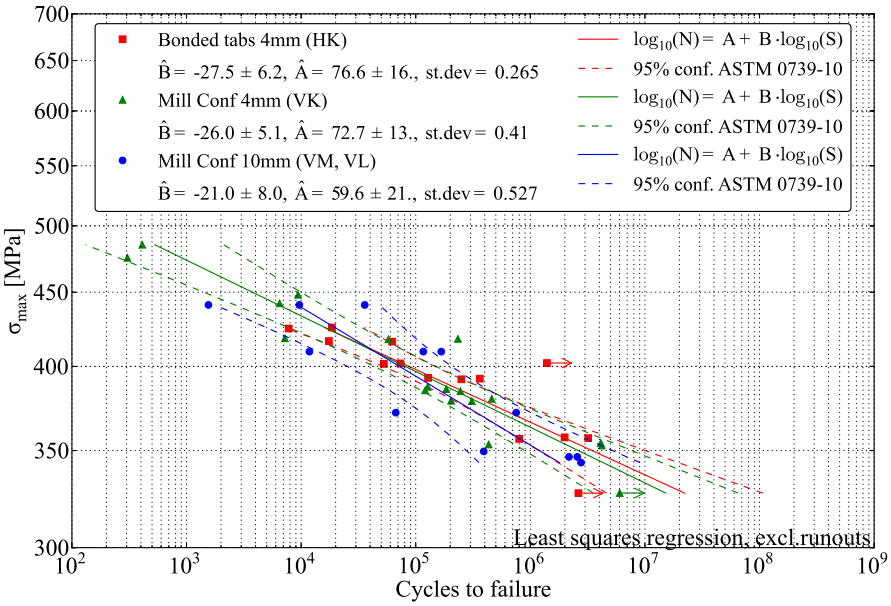

Figure 8: SN-curves (R=10) for 4, 10 and 4 mm R08. Least-square regression.

surement of the Poisson ratios in direction 12 and 13. Table 3 shows that the Poisson ratio in direction 12 is comparable to Poisson ratios in direction 13 for the resin-fibre system tested in this work.

While the scaled geometries did not show a reduction of the ultimate strength due to the thickness, they show a decrease in the fatigue life S-N curves slopes. Figure 8 shows the R=10 S-N curves for 4 mm R08 coupons with bonded tabs, 4 mm milled coupons and 10 mm milled thick coupons. Bonded and milled tabbed 4 mm thick coupons show a similar S-N curve in terms of slopes and intervals of confidences. The 10 mm thick scaled coupons show a reduction of the fatigue life slope from 26 to 21 and an increase of the interval of confidence width. On the other hand, the three curves are located in the same probabilistic interval of confidence thus it can also be argued that there is not enough statistical significance to confirm this trend. Further work is on-going in order to test the coupons with 20 mm thicknesses and higher under fatigue loading conditions.

6. Concluding remarks.

A parametric FEM analysis with cohesive elements was performed in order to design scaled compression coupons showing that when the thickness increases, a stress gradient appears through the thickness.

Static tests of scaled compression coupons for 4, 10 and 20 mm were performed, showing no thickness effect in the ultimate strength. In addition Poisson ratios in directions 12 and 13 were measured showing comparable values. Stress gradients through-the-thickness predicted by FEM models were observed in the tests through strains measurements in the middle and outer xz plane.

While the scaled geometries did not show a reduction of the ultimate strength due to the thickness, they showed a decrease in fatigue life S-N curves slopes with increasing thickness. However, this decrease did not show to be statistically significant for coupons up to 10 mm thick.

Acknowledgements

We acknowledge financial support for this research from ADEM, A green Deal in Energy Materials of the Ministry of Economic Affairs of The Netherlands (www.adem-innovationlab.nl).

References

[1] E Stammes, R.P.L. Nijssen, and T Westphal. Effect of laminate thickness tests on thick laminates. Report WMC-2009-38. Technical Report May, Knowledge centre WMC, Wieringerwerf NL, 2010.

[2] Arno van Wingerde, E Stammes, R.P.L. Nijssen, and T Westphal. 2500 kN test set-up for thick laminates WP10 Optimat blades. Report OB_TG4_R015. Technical report, Knowledge Centre WMC, Knowledge centre WMC, Wieringerwerf NL, 2006.

[3] F Lahuerta, T Westphal, and RPL Nijssen. Self-heating forecasting for thick laminates testing coupons in fatigue. In *The Science of Making Torque from Wind, Torque*, Oldenburg, Germany, 2012.

[4] L S Sutherland, R A Shenoi, and S M Lewis. Size and scale effects in composites: I. Literature review. *Composites Science and Technology*, 59:209–220, 1999.

[5] G Camponeschi. The effects of specimen scale on the compression strength of composite materials. In *Workshop on scaling effects in composite materials and structures NASA-CP-3271*, 1994.

[6] E.M. Odom and D.F. Adams. Failure modes of unidirectional carbon/epoxy composite compression specimens. *Composites*, 21(4):289–296, July 1990.

[7] JG Haberle and FL Matthews. An improved technique for compression testing of unidirectional fibre-reinforced plastics, development and results. *Composites*, 25(5):358–371, 1994.

[8] D F Adams and G A Finley. Experimental Study of Thickness-tapered Unidirectional Composite Compression Specimens. *Experimental Mechanics*, 36(4):345–352, 1996.

[9] H. M. Hsiao, I. M. Daniel, and S. C. Wooh. A New Compression Test Method for Thick Composites. *Journal of Composite Materials*, 29(13):1789–1806, September 1995.

[10] J. Lee and C. Soutis. Thickness effect on the compressive strength of T800/924C carbon fibre epoxy laminates. *Composites Part A: Applied Science and Manufacturing*, 36(2):213–227, February 2005.

[11] I M Daniel and R D Cordes. Dynamic Compressive Behavior of Thick Composite Materials. *Experimental Mechanics*, 38(3):172–180, 1998.

[12] F. Lahuerta, S. Raijmaekers, J.J. Kuiken, T. Westphal, and R.P.L. Nijssen. Automated delamination length video tracking in static and fatigue DCB test. In *6th International Conference on Composites Testing and Model Identification*, pages 6–7, Aalborg, DK, 2013.

[13] F Lahuerta and RPL Nijssen. Static ENF test configuration, with different reinforcement roving configuration. WMC-2013-004c. Technical report, WMC Knowledge Centre, Wieringerwerf, NL, 2013.

[14] Upwind Optidat Database. WMC Knowledge Centre. Technical report, http://www.wmc.eu/optimatblades_optidat.php.